A Stable Ln(III)-Functionalized Cd(II)-based Metal-Organic Framework: Tunable White-Light Emission and Fluorescent Probe for Monitoring Bilirubin

Xiao-Qing Wang*, Xuehui Ma, Doudou Feng, Dan Wu, Jie Yang*

1. X-ray structure determination and structure refinement. The Single-crystal X-ray data of complex **1** were collected on a Bruker Apex II CCD diffractometer using Mo Kα radiation (λ = 0.71073 Å) at 293 K. It adopts the highest possible space group. The structure for **1** was solved by superfilp method using Olex2 program, then refined by full-matrix least-squares on F2 using SHELXL-2016.[S1] All non-hydrogen atoms for **1** were treated anisotropically. The highly disordered free solvent molecules in **1** were removed with the PLATON/SQUEEZE routine.[S2,S3] Its crystal data and refinement parameters were listed in Table 1. The selected bond distanced and angles were shown in Table S1. The Crystal data of complex **1** have been deposited as 1918381 at the Cambridge Crystallographic Data Center.

2. Photoluminescent sensing experiments.

All relevant fluorescence tests were performed at room temperature. For sensing of various metal ions, 2 mg solid power of **1b** was uniformly mixed in 2 mL PBS (pH=7.4) of $M(NO_3)_x$,(M^{x+} = Al^{3+}, Ag^{+}, Ca^{2+}, Cu^{2+}, K^{+}, Mg^{2+}, Na^{+}, Zn^{2+}, CO_3^{2-}, HCO_3^{-}, HPO_4^{2-}, NO_3^{-}, 0.010 mol•L^{-1}). For sening of amino acids, 2 mg solid power of **1b** was uniformly mixed in 2 mL PBS (pH=7.4) of various amino acids, including ascorbic acid (AA), glycine (Gly), methionine (Met), phenylalanire (Phe), cysteine (Cys), bilirubin (BR).

3. Fluorescence Titration experiments.

The 2.0 mg powder sample of **1b** was dispersed in 2.0 mL PBS (pH=7.4) of target analytes with different concentrations.

4. Time-dependent fluorescence sensing experiments.

The fluorescence intensity of **1b** within the BR solutions (1.25 mM) was recorded at 30 s, 60 s, 90 s, 120 s, 150 s, 180 s, 210 s, 240 s, 300 s, 360 s.

5. Recyclable Luminescence Experiments.

The solid powder of **1b** in a centrifuge at 4000 rpm for 20 minutes, then wash the solid powder three times with absolute ethanol, filter and dry, and recovered the solid powder and add the analyte for fluorescence detection. The same operation is performed five times.

Table S1 Selected bond lengths (Å) and angles (°) for complex **1**

Cd3—O6	2.466 (9)	Cd3—O4^{ii}	2.313 (8)
Cd3—O7^{i}	2.569 (13)	Cd3—O5	2.354 (9)
Cd3—O13	2.268 (11)	Cd3—C8^{ii}	2.672 (12)
Cd3—O8^{i}	2.258 (9)	Cd3—C15	2.757 (12)
Cd3—O3^{ii}	2.356 (9)	Cd2—O12	2.222 (13)
Cd2—O2	2.192 (11)	Cd2—O11^{iii}	2.511 (10)
Cd2—O2^{iii}	2.191 (11)	Cd2—O11	2.511 (10)

Cd2—N1	2.40 (2)	Cd1—O1^{iii}	2.261 (9)
Cd1—O12	2.376 (12)	Cd1—N2^{ii}	2.251 (18)
Cd1—O10	2.253 (9)	Cd4—O15^{iv}	2.26 (2)
Cd1—O10^{iii}	2.253 (9)	Cd4—O15	2.26 (2)
Cd1—O1	2.261 (9)	Cd4—O14^{iv}	2.41 (2)
O6—Cd3—O7^{i}	174.4 (4)	O13—Cd3—O6	98.9 (4)
O6—Cd3—C8^{ii}	92.8 (3)	O13—Cd3—O7^{i}	75.7 (4)
O6—Cd3—C15	26.2 (3)	O13—Cd3—O3^{ii}	141.0 (4)
O7^{i}—Cd3—C8^{ii}	88.2 (4)	O13—Cd3—O4^{ii}	88.4 (4)
O7^{i}—Cd3—C15	153.4 (4)	O13—Cd3—O5	87.9 (4)
O13—Cd3—C8^{ii}	115.6 (5)	O8^{i}—Cd3—O3^{ii}	92.9 (4)
O13—Cd3—C15	91.9 (4)	O8^{i}—Cd3—O4^{ii}	131.5 (4)
O8^{i}—Cd3—O6	131.5 (4)	O8^{i}—Cd3—O5	85.8 (4)
O8^{i}—Cd3—O7^{i}	52.6 (4)	O8^{i}—Cd3—C8^{ii}	111.8 (4)
O8^{i}—Cd3—O13	106.0 (5)	O8^{i}—Cd3—C15	111.1 (4)
O3^{ii}—Cd3—O6	92.9 (4)	O3^{ii}—Cd3—O7^{i}	90.4 (4)
Symmetry codes: (i) *x*+1, *y*, *z*; (ii) −*x*+1, *y*+1/2, *z*; (iii) *x*, *y*, −*z*+1/2; (iv) −*x*, −*y*+2, −*z*; (v) *x*−1, *y*, *z*; (vi) −*x*+1, *y*−1/2, *z*.			

Table S2. Hydrogen bonding geometry (Å, º) for complex **1**.

D – H ⋯ A	**D – H / Å**	**H ⋯A / Å**	**D ⋯ A / Å**	**D – H ⋯A / °**
O12-H12A⋯O9	0.85	1.89	2.6489(2)	148
O13^{vi}-H13B^{vi}⋯O7	0.85	2.58	2.9787(3)	110
O13-H13A⋯O5^{v}	0.85	1.87	2.7028(2)	168
O15-H15A⋯O7	0.85	2.08	2.8882(2)	160
Symmetry code: (vi) -1+x, y, z.				

Table S3 The molar ratios of Eu(III) and Tb(III) ions and CIE coordinates of complex **1** soaked in $Eu(NO_3)_3·6H_2O$ and $Tb(NO_3)_3·6H_2O$ for different time.

	Time (h)	Cd(II)/Eu(III) ratio calculated from ICP		Cd(II)/Tb(III) ratio calculated from ICP		CIE
		Cd	Eu	Cd	Tb	
1a	2	0.3677	0.01176	-	-	0.2089,0.2267
	4	0.3375	0.01374	-	-	0.2293,0.2302
	8	0.3415	0.01624	-	-	0.2408,0.2337
	12	0.3321	0.02791	-	-	0.2579,0.2417
	24	0.3431	0.02566	-	-	0.2763,0.2461
	48	0.3306	0.04003	-	-	0.2943,0.2499
1b	2	-	-	0.3496	0.003906	0.3479,0.4723
	4	-	-	0.3631	0.007051	0.3737,0.52
	8	-	-	0.3733	001211	0.3758,0.5237
	12	-	-	0.3371	0.01195	0.3918,0.5373
	24	-	-	0.3375	0.01713	0.3747,0.5202
	48	-	-	0.3226	0.02358	0.3788,0.532

Table S4 The quantum yield and flourescence life time of complexes **1**, **1a**, **1b**, **1b-BR**.

Complex	Quantum yield (%)	Flourescence lifetime (us)				
		τ_1 (us)	τ_2 (us)	a_1	a_2	Average lifetime (us) $<\tau>$*
1	2.24	0.9863	8.3800	0.6263	0.3737	3.749
1a	5.76	1.0449	9.4422	0.6972	0.3028	3.588
1b	13.58	0.9128	7.8833	0.6314	0.3686	3.482
1b-BR	0	0.9941	8.0876	0.6649	0.3351	3.371

$<\tau>^* = \tau_1 a_1 + \tau_2 a_2$

Table S5 The CIE coordinates of the **1** suspended solutions with varying the Eu: Tb molar ratio (5:0 to 5:60)

Eu(III)/Tb(III)	CIE
0	0.1772, 0.2405
5: 0	0.2369, 0.2481
5: 5	0.2553, 0.2624
5: 10	0.2634, 0.2719
5: 14	0.2725, 0.2821
5: 25	0.2815, 0.2954
5: 40	0.2892, 0.3074
5: 60	0.3011, 0.3265

Table S6. Performance of materials for detecting BR

	materials	Liner Range (μM/L)	Detection limit	Ref.
1	1b	0-17.5	0.250 μM/L	This work
2	UiO-66$(COOH)_2$:Eu	0-15	0.450 μM/L	35
3	Tb^{3+}@MOF-8080.4−30	0.4-30	0.0260 μM/L 0.0230 μM/L 0.0310 μM/L	S4
4	UIO-66-PSM	10^{-7}-500	0.590 pmol/L	S5
5	Al-MIL-53-NH_2@THB	10^{-6}-12	1.26 pM/L	S6
6	Eu-MOFs	0-56.6	1.75 μM/L	S7

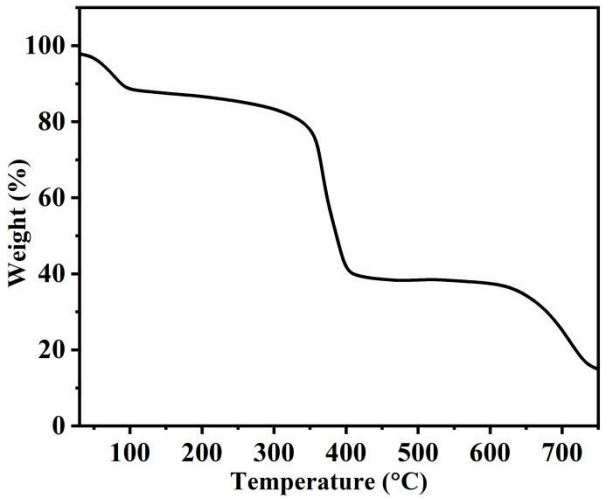

Fig. S1. The TGA curve of complex **1**.

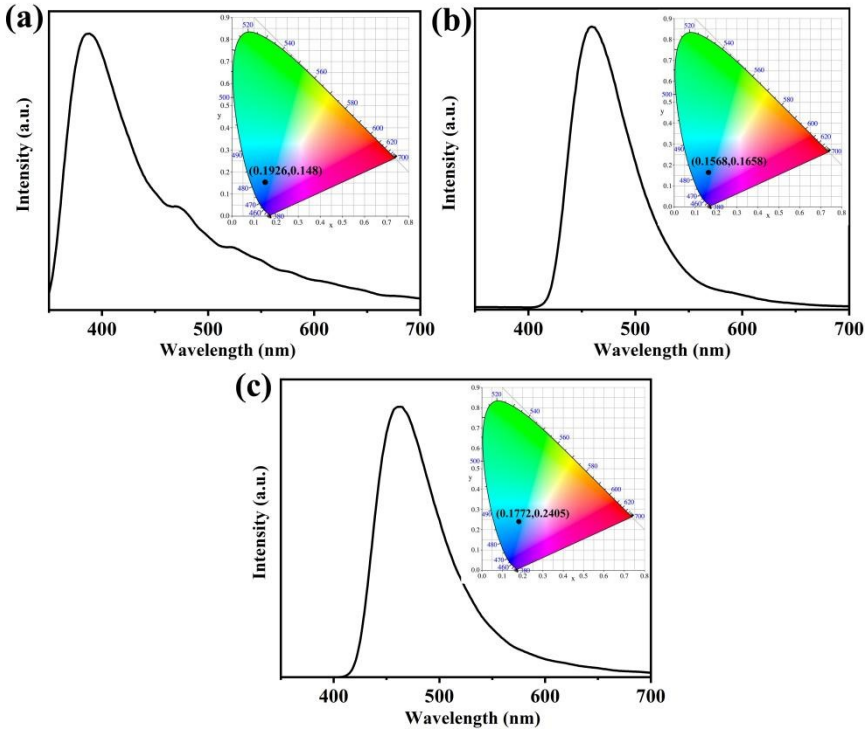

Fig. S2. The solid-state emission spectra of H_5DDB (a), BPP (b) and complex **1** (c) (Inside is the CIE chromaticity diagram).

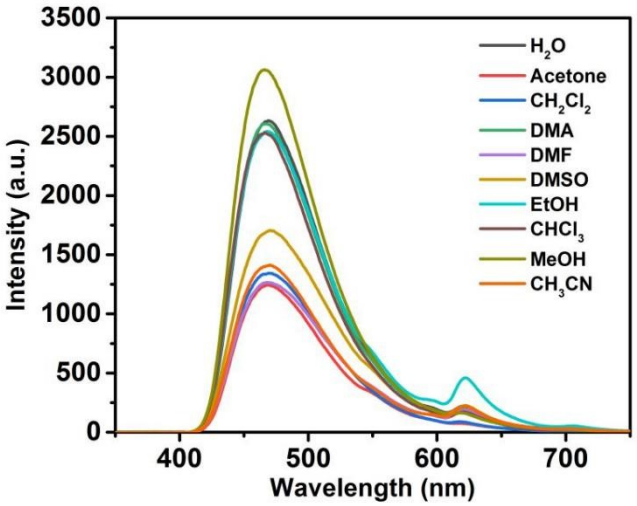

Fig. S3. The liquid-state emission spectra of complex **1** in different solvents at 298 K.

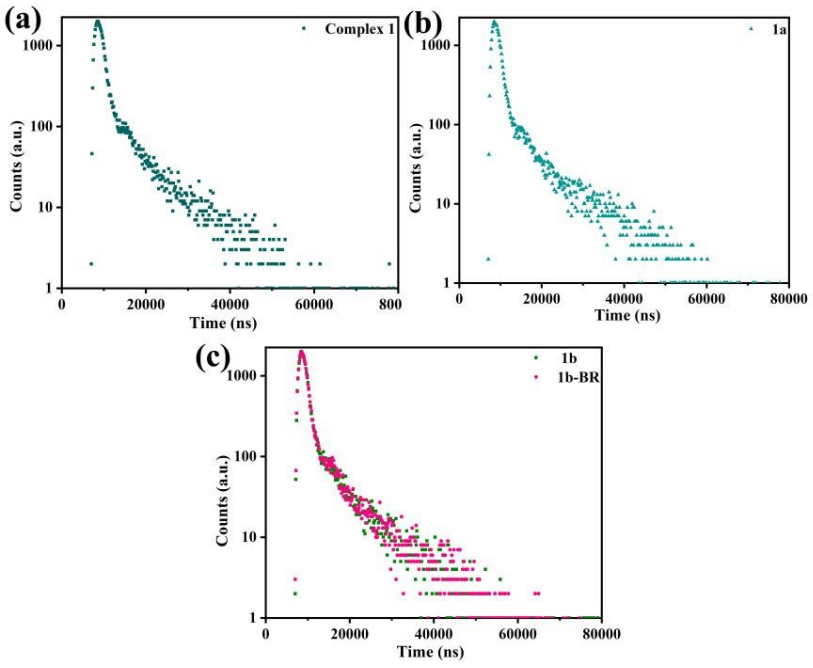

Fig. S4. Lifetime decay profile of complex **1** (a), **1a** (b), **1b** and **1b-BR** (c).

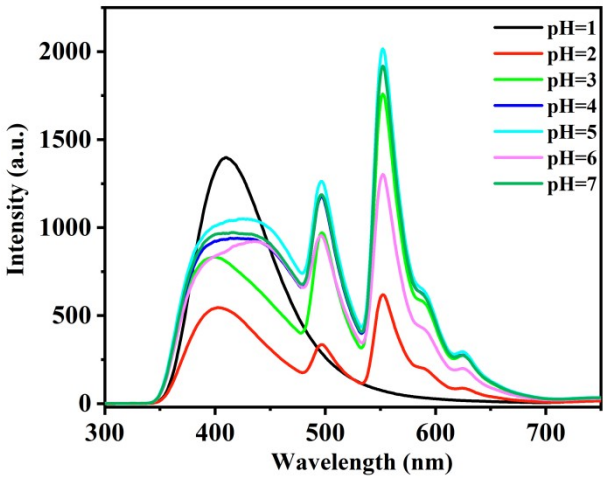

Fig. S5. Fluorescence properties of **1b** suspension at different pH.

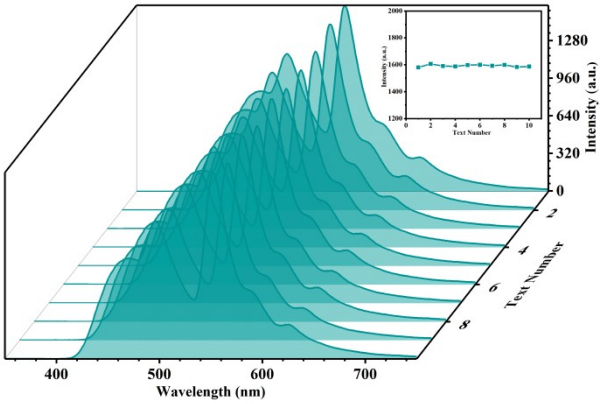

Fig. S6. The fluorescence intensity of 1b was measured 10 times in water.

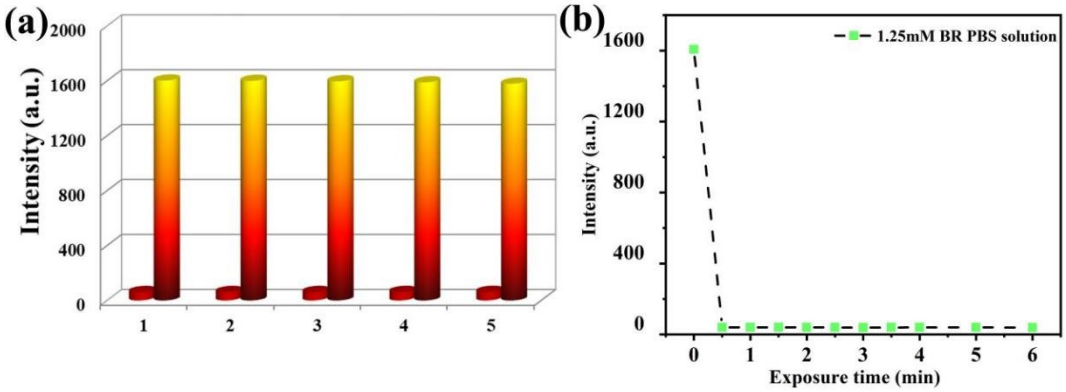

Fig. S7. (a) The luminescence intensity of **1b** for detecting BR after five cycles. (b) The fluorescence intensity of **1b** in BR solution as a function of exposed time.

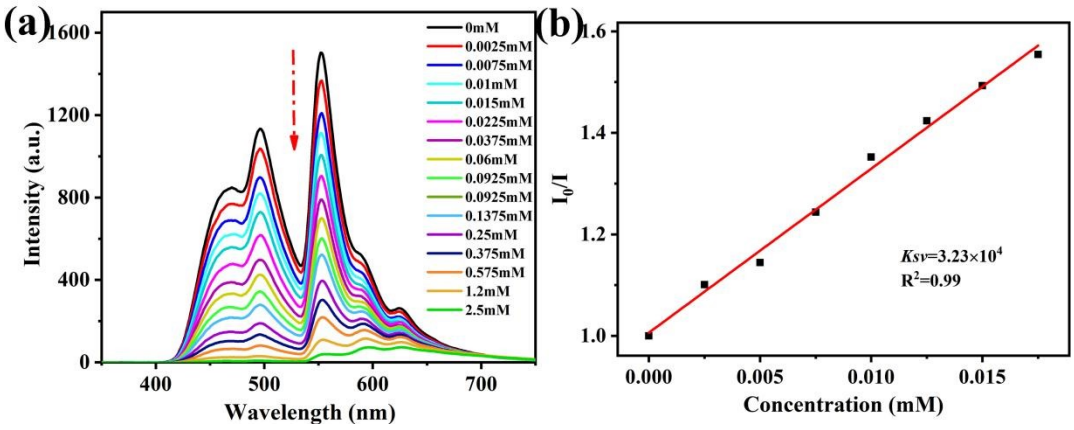

Fig. S8. (a) Titration curve of **1b** to BR in human serum. (b) SV plot of **1b** for sensing of BR in human serum.

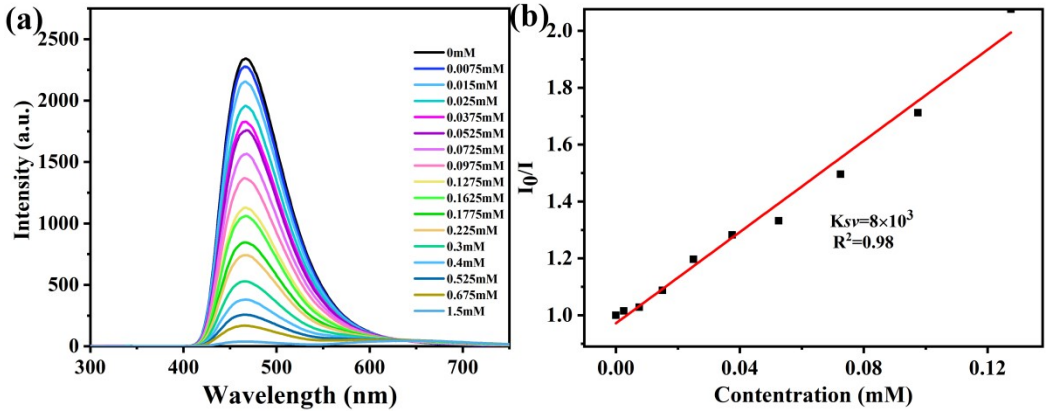

Fig. S9. Titration curve of **1** to BR in PBS. (b) SV plot of **1** for sensing of BR in PBS.

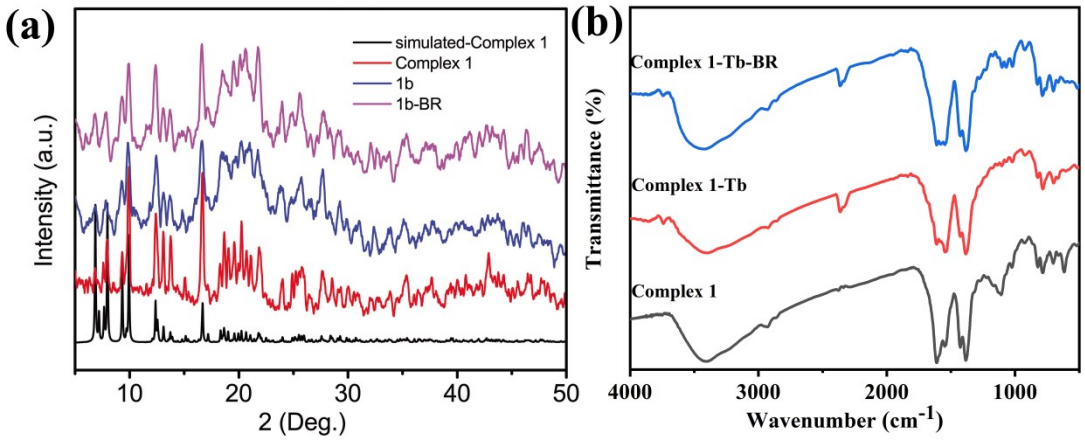

Fig. S10. (a) PXRD patterns of complex **1** before and after exposure to different analytes. (b) The IR patterns of complex **1** before and after exposure to different analytes.

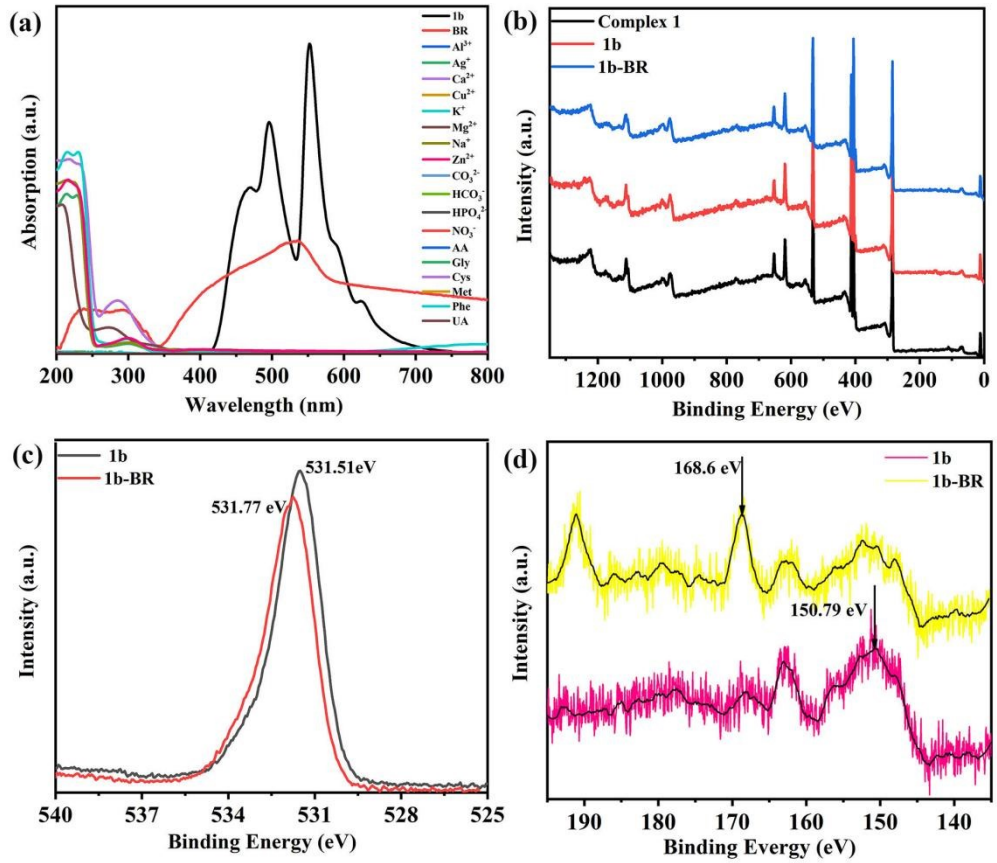

Fig. S11 (a) The fluorescence emission spectra of **1b** and the UV-vis absorption spectra of various metal ions and amino acids. (b) XPS spectra of complex **1**, **1b** and **1b**-BR. (c) XPS spectra of O 1s for **1b** and **1b**-BR. (d) XPS spectra of Tb 4d for **1b** and **1b**-BR.

Reference

S1. Sheldrick, G. M. Crystal structure refinement with SHELXL. *Acta Cryst. C*.,**2015**, *71*, 3-8.

S2. Speck, A. L. PLATON. a multipurpose crystallographic tool, Utrecht University. Utrecht. *The Netherlands*, **2001**.

S3. Spek, L .A. Multipurpose crystallographic tool. *J. Appl. Crystallogr*. **2003**, *36*,7-13.

S4. K. Y. Yi, H. Li, X. T. Zhang and L. Zhang, *Inorg. Chem.*, 2021, **60**, 3172-3180

S5. Y. R. Du, X. Q. Li, X. J. Lv and Q. Jia, *ACS Appl. Mater. Inter.*, 2017, **9**, 30925-30932.

S6. S. Nandi and S. Biswas, *Dalton Trans.*, 2019, **48**, 9266-9275.

S7. P. Xu, H. W. Yang, J. L. Shi, B. Ding, X. J. Zhao and E. C. Yang, *RSC Adv.*, 2019, **9**, 37584-37593.